Optics Communications 285 (2012) 171–177

Contents lists available at SciVerse ScienceDirect

Optics Communications

journal homepage: www.elsevier.com/locate/optcom

Soliton propagation optimization and dynamic modulation in photonic crystal waveguide with polystyrene background

Lingyu Liu, Daquan Yang, Huiping Tian, Yuefeng Ji *

Key Laboratory of Information Photonics and Optical Communications, Ministry of Education, School of Information and Telecommunication Engineering, Beijing University of Posts & Telecommunications, Beijing, PR China

ARTICLE INFO

Article history:
Received 23 March 2011
Received in revised form 25 August 2011
Accepted 26 August 2011
Available online 12 September 2011

Keywords:
Optical soliton
Photonic crystal waveguide
Dynamic modulation
Peak power
Delay time

ABSTRACT

Bright optical soliton propagation properties near the left band edge of photonic crystal waveguide (PCW) are numerically investigated. Compared with the normal PCW with air background, by employing polystyrene as PCW background and adjusting the structure parameters simultaneously, the required soliton peak power sharply decreases from 8.63×10^6 W/m to 9.98×10^2 W/m. The influence of optical loss on soliton propagation is numerically investigated. The dynamic modulation of the soliton propagation in PCW is realized, and a modulation range of 459 nm wavelength for the soliton transmission has been achieved. Simulation results show that the transmission wavelength, required soliton peak power and delay time decrease almost linearly as the external modulated voltage increases; the modulation sensitivities are 8.316 nm/V, 3.416 W/m/V and 16.6 ps/V, respectively.

1. Introduction

In photonic crystal waveguide(PCW), the periodic lattice structure leads to extremely strong material dispersion; thus the group velocity of the guided modes that in the photonic band gap (PBG) will be substantially reduced which caused slow light [1]. Slow light based on PCW has been a research focus in optical communications due to its broad range of applications, such as optical delay lines, highly nonlinear devices, all-optical buffer and etc. [2–8].

However, the slow light region near the photonic band edge is usually accompanied by large group velocity dispersion (GVD) which severely deforms the optical pulses of high speed optical signals severely, and thus disturbs its practical application. In the linear regime [3,7–11], the main method to solve the large GVD is to realize tailored negligible dispersion or dispersion compensation [3,7–11]; even so, the maximum bit rate which can be achieved at a specified delay is still considerably limited [10]. Benjamin J. Eggleton has first reported the nonlinear optical pulse compression and soliton propagation in fiber Bragg gratings, which showed that solitons can be formed in periodic structures [12]. A relevant amount of work about Bragg solitons in fiber Bragg gratings has been investigated by Benjamin J. Eggleton et al. [13–15]. The results of Thomas Kamalakis et al's studies [16–18] show that the soliton can be supported in photonic crystal coupled resonator optical waveguides(CROW) [17] and near the band edge of line PCW, theoretically [18]. Moreover, Colman et al. have experimentally demonstrated the optical soliton compression in slow-light photonic crystal waveguide [19,20]. Christelle Monat et al. have also experimentally studied that various nonlinear phenomena are enhanced due to slow light in silicon photonic crystal waveguides [21]. All these works and results show that using soliton pulses as information carriers in the nonlinear regime has opened a new way towards exploiting the low group velocity that PCW has exhibited. Soliton communication is especially appealing in optical network for its advantages. However, Thomas Kamalakis et al's work only focused on soliton propagation in the conventional PCW [16–21]; actually, the required soliton peak power can be further reduced by optimizing. Moreover, for practical application, the controllable all-optical devices are the most critical components [22]. For this reason, it is quite necessary to realize the dynamic modulation of the soliton propagation in PCW.

In this paper, we investigate the soliton propagation properties of a line defect PCW with polystyrene background. Firstly, we focus on optimizing the soliton propagation performance of the PCW by appropriately adjusting the structure of the waveguide. Then, the influence of optical loss on soliton propagation in PCW is examined. Lastly, the soliton propagation dynamic modulation realized by external voltage is discussed, including transmission wavelength, the required soliton peak power and delay time.

* Corresponding author at: P.O. Box 90, BUPT, No. 10, Xitucheng Road, Haidian District, Beijing, 100876 PR China.
E-mail addresses: liulingyu0521@163.com (L. Liu), yangdq5896@163.com (D. Yang), hptian@bupt.edu.cn (H. Tian), jyf@bupt.edu.cn (Y. Ji).

0030-4018/$ – see front matter
doi:10.1016/j.optcom.2011.08.066

2. The theoretical model

2.1. The model of the nonlinear pulse propagation in PCW

The propagation of optical pulses inside a PCW follows the following equation [18,23]:

$$j\left(\frac{\delta A}{\delta z}+\frac{\Gamma A}{2}\right)+\sum_{l\geq 2} j^{m(l)}\frac{\beta_l \delta^l A}{l!\delta T^l}+\gamma|A|^2 A=0 \quad (1)$$

Eq. (1) can describe the pulse evolution as it propagates along the PCW. A is the envelope of the electric field along the PCW. The coefficient Γ is related to the optical losses, and$z$ is the propagation distance. The function $m(l)$ is defined as $m(l)=\mathrm{mod}(l,2)$, while the coefficient β_l is the group velocity dispersion coefficient (for $l=2$) or a higher order dispersion coefficient (for $l>2$).

The GVD parameter is given by [1]

$$\beta_2=\frac{d\left(v_g^{-1}\right)}{d\omega}=\frac{1}{c}\frac{dn_g}{d\omega}=\frac{d^2k}{d\omega^2} \quad (2)$$

where ω is the normalized frequency, k is the wave vector, c is the light velocity in vacuum and v_g is the group velocity which can be obtained by the slope of the guide mode as

$$v_g=\frac{\partial\omega}{\partial k}=\frac{c}{n+\omega\frac{dn}{d\omega}}=\frac{c}{n_g} \quad (3)$$

where $n_g=n+\omega(dn/d\omega)$ is the group index.

The delay time is given by [3]

$$\mathrm{Ts}=\frac{L}{v_g}=\frac{n_g}{c}\times L \quad (4)$$

where L is the length of PCW.

The coefficient γ is the SPM coefficient which can be calculated using [18]

$$\gamma=\frac{2\omega_0}{a}\int_{S_W} dS\varepsilon_{NL}|e_0|^4 \quad (5)$$

The constant a is the period of the lattice along the z-direction, S_W is the area of the unit cell, ande_0 is the y-component Bloch function of the electric field. The PWE method can be used to calculate e_0 in the entire unit cell. ε_{NL} is the nonlinear dielectric constant given by [18]

$$\varepsilon_{NL}(r)\cong 2\varepsilon_0 n n_2(r)(\varepsilon_L(r)/\mu)^{1/2} \quad (6)$$

In Eq. (6), ε_0 is the dielectric constant of vacuum, n is the refractive index of the dielectric, n_2 is the nonlinear refractive index and μ is the magnetic permeability. Numerically integrating $\varepsilon_{NL}|e_0|^4$ over the entire cell, the value of γ is calculated.

Near the left band edge of PCW, $\beta_2<0$, bright solitons are supported; the initial condition for the bright soliton solution is [18,23]

$$A(0,T)=\sqrt{P_0}\sec h(T/T_0) \quad (7)$$

where T_0 is the initial soliton width determined by $T_0\approx t_{FWHM}/1.76$, t_{FWHM} is the FWHM of the pulse and P_0 is the required soliton peak power, determined by

$$P_0=\frac{|\beta_2|}{\gamma T_0^2} \quad (8)$$

Substitute $t_{FWHM}=1/4R_b$ into Eq. (8); Eq.(8) can be rewritten as

$$P_0\cong 49.5\frac{|\beta_2|}{\gamma}R_b{}^2 \quad (9)$$

where γ *is* the SPM coefficient, β_2 is the GVD parameter, and R_b is the bit rate of the signal.

2.2. The PCW model

The PCW we research consisting of a single line defect and triangular lattice Si-rods is illustrated in Fig. 1. The nonlinear refractive index of Si rods is $n_{2\text{-Si}}=1.5\times10^{-16}\ \mathrm{m^2/W}$ [18]. As shown in the figure, the background material of PCW is polystyrene, which has both high nonlinear refractive index n_2 and large electro-optic coefficient γ_{33}. The nonlinear refractive index of polystyrene is $n_{2\text{-polystyrene}}=-9.3\times10^{-13}\ \mathrm{m^2/W}$ [24], which is much larger than that of the frequently used nonlinear materials in photonic crystals. For example, the nonlinear refractive index of GaAs is $n_{2\text{-GaAs}}=1.6\times10^{-17}\ \mathrm{m^2/W}$ [25], and that of GaInP is $n_{2\text{-GaInP}}=8\times10^{-18}\ \mathrm{m^2/W}$ [26]. Thus the SPM coefficient γ can be improved due to the large value of $n_{2\text{-polystyrene}}$. In addition to the large nonlinear refractive index $n_{2\text{-polystyrene}}$, the polystyrene also has a high electro-optic coefficient (10 pm/V to 170 pm/V) [27], which can be used to realize electro-optic modulation. The refractive indexes of the Si and polystyrene are 3.5 and 1.59.

In this paper, the optimization of the soliton propagation performance is achieved by adjusting some PCW structure parameters. As shown in the figure, the lattice constant is a. The radius of the first two rows of rods adjacent to the defect is denoted by r_1, the second two rows' is r_2 and the remaining rows' is r. Δx_1 and Δx_2 represent the shifted along waveguide axis of the first and second two rows adjacent to the defect, respectively. The width of the common waveguide is D. The width of the waveguide becomes d by moving the first two rows of air-holes symmetrically.

3. Optimization of bright soliton propagation performance in PCW

Within our work, several PCW structure parameters have been adjusted to achieve the optimization of bright soliton transmission performance. The main criterion which has been followed during the optimization is that the required soliton peak power P_0 is reduced. By changing the PCW structure parameters, the shape of the guided mode changed, so the properties of the guided mode such as the group velocity, group velocity dispersion and field distribution changed accordingly, which finally leads the change of the required peak power P_0 for soliton propagation in PCW. The structure parameters r, r_1, r_2, Δx_1, Δx_2, and d are adjusted to obtain the reduction of the required peak

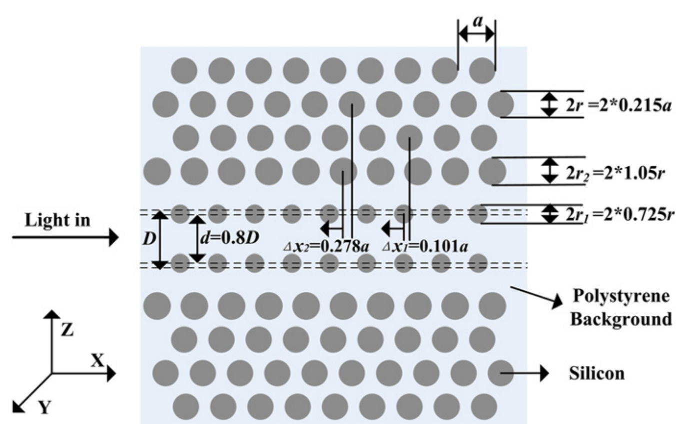

Fig. 1. Schematic of the line defect PCW with Si-rods and polystyrene background.

power P_0. The optimized PCW structure is shown in Fig. 1; the parameters are $r=0.215a$, $r_1=0.725r$, $r_2=1.05r$, $\Delta x_1=0.101a$, $\Delta x_2=0.278a$, $d=0.8D$, and $D=\sqrt{3}a$.

The typical band diagram for TM-like polarized light in PCW is obtained and shown in Fig. 2. The properties of PCW are calculated by using the plane-wave expansion (PWE) method. The defect mode inside the band gap is studied by replacing a 1×10 unit cell with a supercell that is 1 unit in the X-direction and 10 units in the Z-direction in the PWE calculation, as shown in the upper left inset of Fig. 2. In simulation analysis, the wave vector K is normalized wave vector, and frequency is normalized frequency $\omega a/2\pi c$. As seen, the PCW supports only a single guided mode in PBG, which is the result we pursued.

Fig. 3 sketches the group index and group velocity dispersion of the PCW. The small value of K represents the left edge of guide mode. It can be seen that there is a large increase in n_g near the left band edge of the guided mode. The GVD curve indicates that the dispersion relation is such $\beta_2<0$ near the left band edge, so the bright soliton can be considered in PCW [18].

In this paper, we focus on the slow light based on the bright soliton pulse propagation at the wave vector point $K_0=0.01389$ where near the left band edge of PCW with polystyrene background. It can be calculated that the group index is $n_g\approx69$ and the group velocity dispersion is $\beta_2\approx-2.71\times10^8$ ps^2/km at $K_0=0.01389$. The lattice constant a is chosen to be 438 nm so that the wavelength of K_0 is 1550 nm. The required soliton peak power P_0 and delay time Ts are used to estimate the soliton transmission performance. P_0 and Ts are calculated by using Eqs. (9) and (4), separately. Fig. 4. illustrates the relation between the required soliton peak power density P_0 and the bit rate of the signal R_b of the PCW. It can be seen that P_0 becomes larger with the increase of R_b.

Now, have a look in detail at how the soliton performance can be improved by using polystyrene as PCW's background and adjusting the structure parameters. Actually, an optimized PCW with air background and Si rods for soliton propagation has been got in our previous research work [28].

Here, in order to describe it more clearly, Table 1 gives a comparison between the PCW with polystyrene background (PCW-P) in this paper and the PCW with air background (PCW-A) in Ref.[28]. The structure parameters and soliton performance of two PCWs (when $R_b=100$ Gb/s, waveguide length $L=1$ cm) are shown in Table 1. As shown in the table, the two PCW structures have the same group index $n_g=69$, while compared with PCW-A, P_0 of PCW-P has a significant reduction and sharply decreases from 8.63×10^6 W/m to 9.98×10^2 W/m, which has got a 8.65×10^3 times reduced. This is mainly due to the fact that the nonlinear refractive index of polystyrene is much larger than that of air. It reveals that the soliton propagation in PCW-P is much better than that in PCW-A, yet has the same slow light delay time Ts = 2.3 ns. Meantime, the SPM coefficient γ of PCW-P is 7.47×10^3 times larger than that of PCW-A. All the results indicate that the soliton performance is effectively improved in our proposed structure.

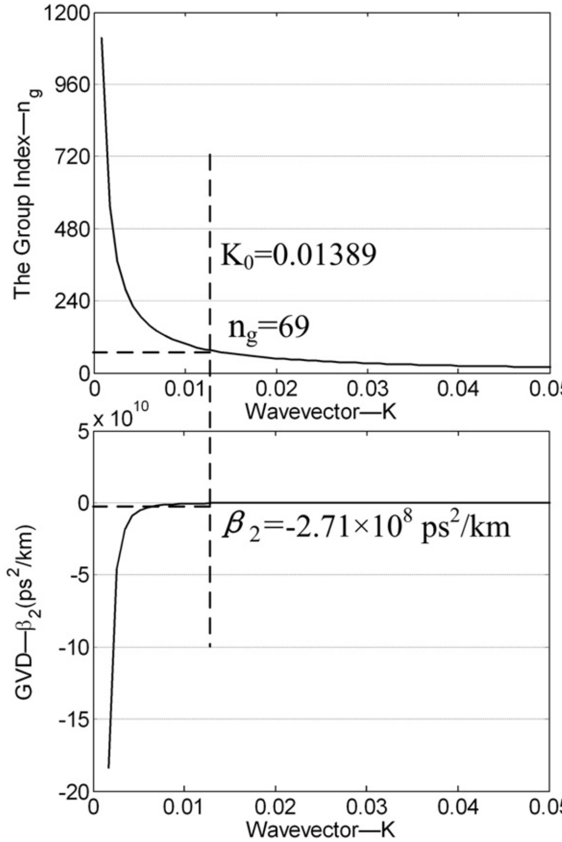

Fig. 3. Group index n_g and group velocity dispersion β_2 near left band edge of the guided mode of PCW.

The soliton propagation waveform in PCW and the normalized electric field of the supercell are also numerically investigated. Fig. 5(a) shows the bright soliton propagation without higher order dispersion effects and optical loss in PCW. The distance is in the unit of the dispersion length L_D, and the length of PCW is $L=1$ cm; thus the distance is $L=1343\times L_D$ after calculating. As shown in the figure, the soliton pulse propagates without waveform distortion. Consequently, it is

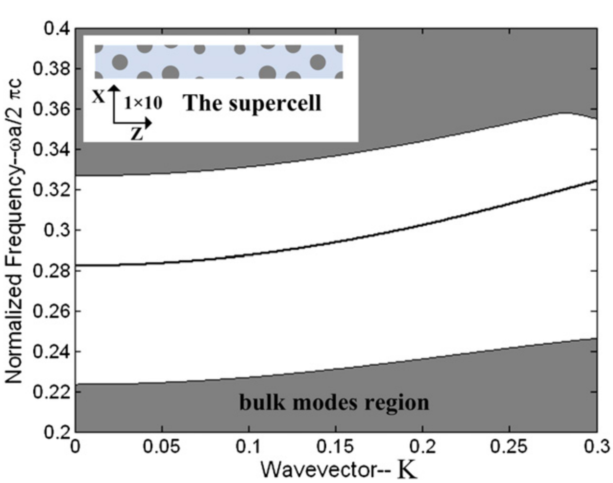

Fig. 2. Photonic band of the PCW for the TM-like polarization. The upper left inset sketches the supercell used in PWE calculation.

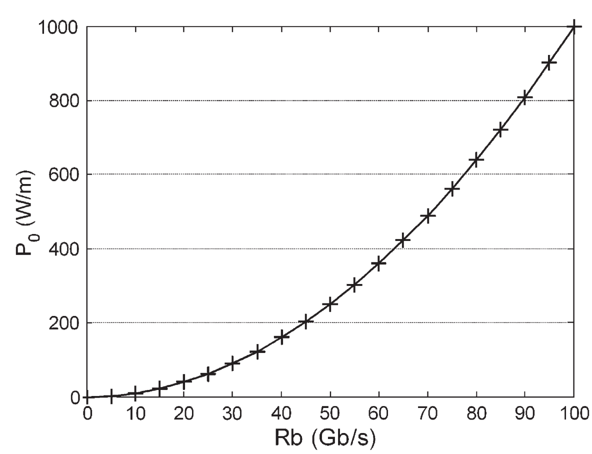

Fig. 4. Required soliton peak power density P_0 as a function of the bit rate of the signal R_b in PCW.

Table 1
The structure parameters and soliton performance of the two PCWs.

Structure	Structure parameters							Soliton performance			
	a (nm)	r (a)	r_1 (r)	r_2 (r)	d (D)	Δx_1 (a)	Δx_2(a)	P_0 (W/m)	Ts (ns)	n_g	γ (W^{-1})
PCW-P	438	0.215	0.725	1.05	0.8	0.101	0.278	9.98×10^2	2.3	69	134.37
PCW-A	472	0.25	1.2	1	0.8	0	0	8.63×10^6	2.3	69	0.018

especially appealing in optical communications. Fig. 5(b) is normalized electric field in the supercell of PCW. It can be seen that the local of the electric field is well, which suggests that the soliton pulse signal can propagate effectively in PCW.

In the above analysis, the optical loss was assumed negligible. In practical application, optical loss exists in PCW; thus it is necessary to study the effects of optical loss on soliton propagation performance. The influence of optical loss can broaden the soliton pulse, and the broadening factor BF of soliton pulse is calculated to evaluate the soliton stability in the presence of loss; it is given by Ref. [18]

$$BF(z) = \frac{B_{3dB}(z)}{B_{3dB}(0)} \tag{10}$$

where $B_{3dB}(z)$ is the calculated FWHM of the soliton envelope $A(z,t)$.

Fig. 6 sketches the broadening factor BF_{LOSS} of the bright soliton when taking optical loss into account in PCW-P, when R_b is 100 Gb/s. As shown in the figure, it is concluded that soliton pulses are sensitive to loss, and BF_{LOSS} increases almost linearly as the optical loss increasing. A 33% broadening obtained for Γ is 3 dB/m, so it reveals that the optical loss must now be kept smaller than 3 dB/m in order to avoid pulse broadening beyond 33% [18]. Fig. 7 presents the bright soliton pulse propagation in PCW-P when Γ is 3 dB/m, and R_b is 100 Gb/s.

4. Dynamic modulation of soliton propagation in PCW

For practical application, it is important to recognize that the soliton propagation can be controlled by an external command. Among the available materials for photonic applications, the polymers have attracted great interests due to their high electro-optic coefficient (10 pm/V to 170 pm/V) [27] and fast response time. In addition, the electro-optic effect can be greatly enhanced in the PCW with low group velocity. Due to this fact, we combine the highly nonlinear characteristics of polymers with the good high-index guiding properties of silicon structure to achieve the dynamic modulation of soliton propagation in PCW. Two electrodes have been placed on each side of PCW as shown in Fig. 8. This means that the electrostatic field lines are parallel to the Z axis, allowing the large electro-optic coefficient γ_{33} in polystyrene to be used [29].

4.1. Electro-optic effect enhanced in PCW

In the presence of an external voltage, the refractive index of polystyrene is affected by Pockels effect, which relates to second order susceptibility $\chi^{<2>}$. In PCW with slow light, the nonlinear effects can be greatly enhanced [27,29], which is due to the compression of local density of states. The refractive index of variation of PCW with slow light is generally calculated as [3,30]

$$\Delta n = -\frac{1}{2}\times n_{poly}^3 \times \gamma_{33} \times f^3 \times \frac{U}{d} \tag{11}$$

In Eq. (11), U is the external modulated voltage, d is the distance between the electrodes, γ_{33} is the electro-optic coefficient, and f is the local-field factor in PCW caused by slow light; it can be calculated as [27,29]

$$f = \sqrt{\frac{v_g^{BULK}}{v_g^{PC}}} \tag{12}$$

where v_g^{BULK} is the group velocity in the bulk polystyrene, and v_g^{PC} is the group velocity in the PCW. In our work, we put $\gamma_{33} = 80$ pm/V, for PCW structure, $n_{poly} = 1.59, d = 3.1$ μm. Substituting $v_g^{PC} = c/69$ into Eq. (12), the local-field factor f is calculated to be 6.6.

4.2. Dynamic modulation of the soliton transmission in PCW

Fig. 9 plots the shift of the guided mode due to different applied modulated voltages. As shown, the guided mode shifts to higher frequency with the increasing of applied modulated voltage. The maximum modulation voltage for PCW is calculated to be 55 V, as the

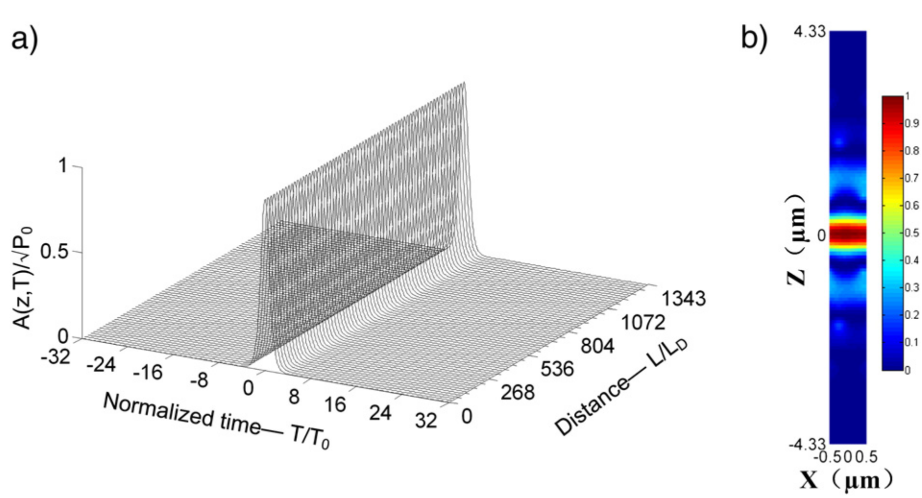

Fig. 5. (a) Bright soliton propagation in PCW; (b) normalized electric field of the supercell.

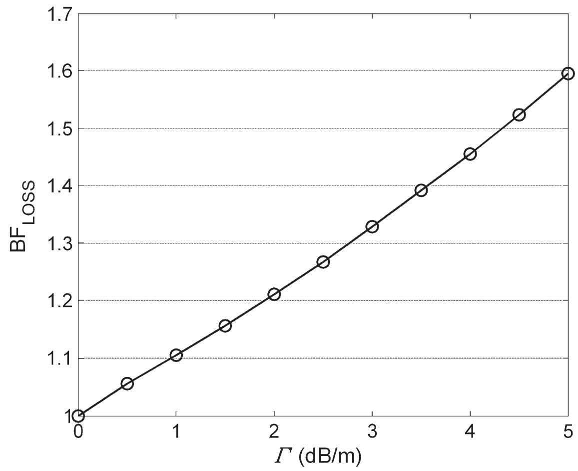

Fig. 6. Broadening factor for soliton pulse with the consideration of loss in PCW-P, $R_b = 100$ Gb/s, $L = 1$ cm.

results show that the frequency of wave vector K_0 is not in the PBG of PCW when the modulated voltage $U > 55$ V. It can be seen that when the applied modulated voltage U is 0 V, 10 V, 20 V, 30 V, 40 V, 50 V and 55 V, the normalized center frequency is 0.28227, 0.29770, 0.31546, 0.33592, 0.35951, 0.38647 and 0.40098, respectively. These results indicate that the shift of guided mode can be tuned by changing the voltage externally. Therefore this characteristic can be applied to manipulate the slow light based on soliton pulse with given frequency dynamically and conveniently.

In order to describe the modulation property more clearly, Fig. 10 plots the wavelength of soliton pulse as a function of applied modulated voltage. It can be seen that the wavelength decreases almost linearly as the applied voltage increasing. Thus, more refined mode shift can be obtained by tuning the voltage more exactly when $U \leq 55$ V. The modulation sensitivity is about 8.316 nm/V. When $U = 55$, the wavelength of soliton pulse is 1091 nm, so it is concluded that the electro-optic modulation of PCW has realized a wavelength range of

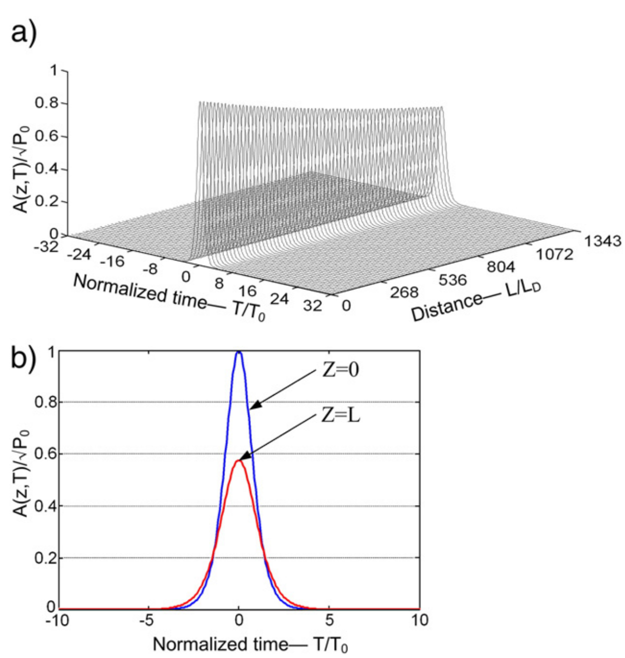

Fig. 7. (a) Bright soliton pulse propagation in PCW-P for $\Gamma = 3$ dB/m, $R_b = 100$ Gb/s; (b) pulse shape at $z = 0$ and $z = L = 1$ cm.

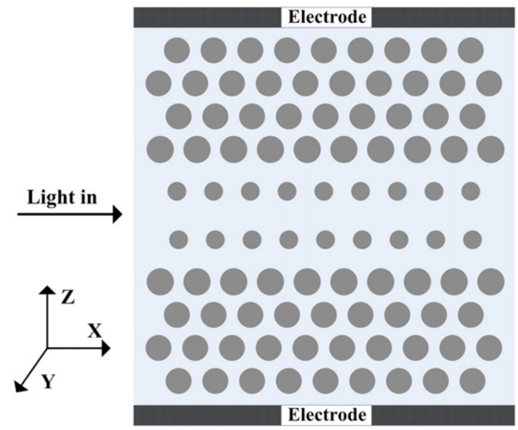

Fig. 8. Schematic configuration of dynamic modulation in PCW.

459 nm for the soliton transmission, which has covered the whole wavelength range of conventional optical communications.

Furthermore, changes in GVD β_2, SPM coefficient γ and group index n_g with the increasing of applied modulated voltage can occur as well, which are also studied and shown in Fig. 11. Fig. 11(a) indicates the GVD β_2 and SPM coefficient γ as a function of applied modulated voltage; it is found that both the values of $|\beta_2|$ and γ decrease with the increase of the modulated voltage. The more detailed calculations of n_g and $|\beta_2|/\gamma$ are shown in Fig. 11(b). Thence, according to Eqs. (4) and (9), it is easy to get the conclusion that the delay time Ts and soliton required peak power P_0 have the same changes trend with that of n_g and $|\beta_2|/\gamma$.

The change trend of the required soliton peak power P_0 and delay time Ts as modulated voltage increasing is shown in Fig. 12. When the modulated voltage U is 0 V, 10 V, 20 V, 30 V, 40 V and 50 V, the required soliton peak power P_0 is 998.3 W/m, 951.9 W/m, 911.7 W/m, 875.8 W/m, 843.7 W/m, and 827.5 W/m, and the delay time is 2.32 ns, 2.12 ns, 1.93 ns, 1.76 ns 1.61 ns, and 1.49 ns respectively. The results suggest that both P_0 and Ts decrease as modulated voltage increases, which is caused by the decrease of $|\beta_2|/\gamma$ and n_g, separately. ComparingFig. 12 with Fig. 11(b), it could be easily found that the changes in the curves of P_0 and $|\beta_2|/\gamma$ are exactly identical, and the same situation occurs between Ts and n_g. When modulated voltage $U \leq 50$ V, it can be seen that both P_0 and Ts decrease almost linearly as U increased, and the modulation sensitivities of P_0 and Ts are about 3.416 W/m/V and 16.6 ps/V, respectively. Thus, for the given PCW, the required soliton peak power and delay time can be controlled flexibly by adjusting the applied modulated voltage accurately.

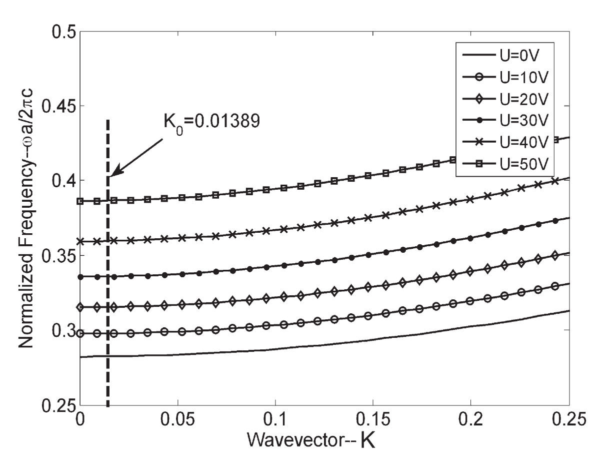

Fig. 9. Guided mode shift as the modulated voltage increasing.

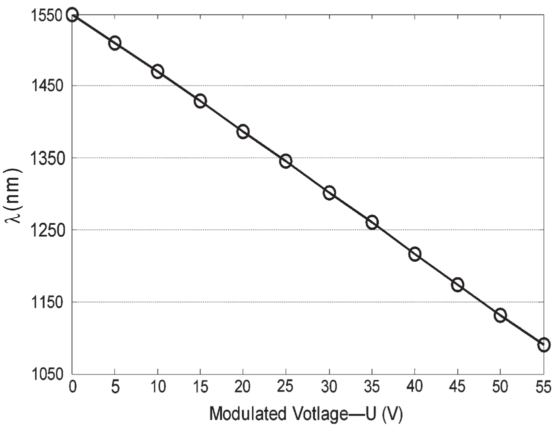

Fig. 10. Wavelength of soliton pulse as a function of applied modulated voltage.

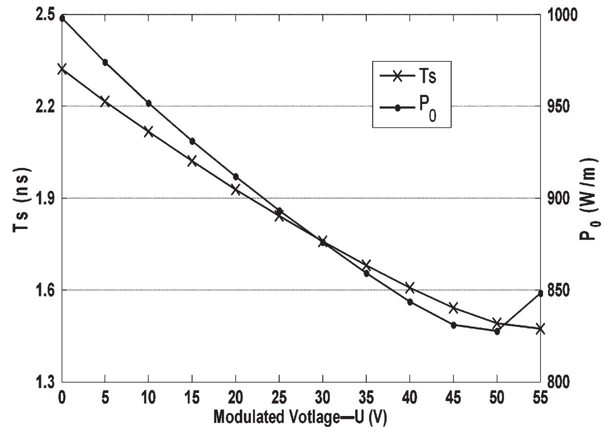

Fig. 12. Required soliton peak power P_0 and delay time Ts as the modulated voltage increases.

It is interesting to note that when $U > 50$ V, P_0 increases with the increase of U, which is mainly due to the properties changes of the guided mode.

5. Conclusion

In summary, by using the polystyrene material which has both high nonlinear refractive index n_2 and large electro-optic coefficient γ_{33} as the background of PCW, we have not only achieved the optimized high-performance bright optical soliton propagation in PCW, but also realized the dynamic modulation of the soliton propagation. After adjusting the parameters of the proposed structure, compared with the PCW with air background, the required soliton peak power sharply decreases from 8.63×10^6 W/m to 9.98×10^2 W/m, while the delay time remains unchanged as Ts = 2.3 ns when $L = 1$ cm. The influence of optical loss on soliton propagation is numerically investigated. The simulation results indicate that the optical loss should be kept smaller than 3 dB/m in order to avoid pulse broadening beyond 33% in our proposed PCW for $L = 1$ cm. Moreover, a wavelength modulation range of 459 nm for the soliton transmission has been achieved, which covers the whole wavelength range of conventional optical communications. The simulation shows that the wavelength, required soliton peak power and delay time decrease almost linearly as the external voltage increases; the modulation sensitivities are about 8.316 nm/V, 3.416 W/m/V and 16.6 ps/V, respectively. These results provide an important theoretical basis for the high-performance soliton application based on PCW in optical communication network.

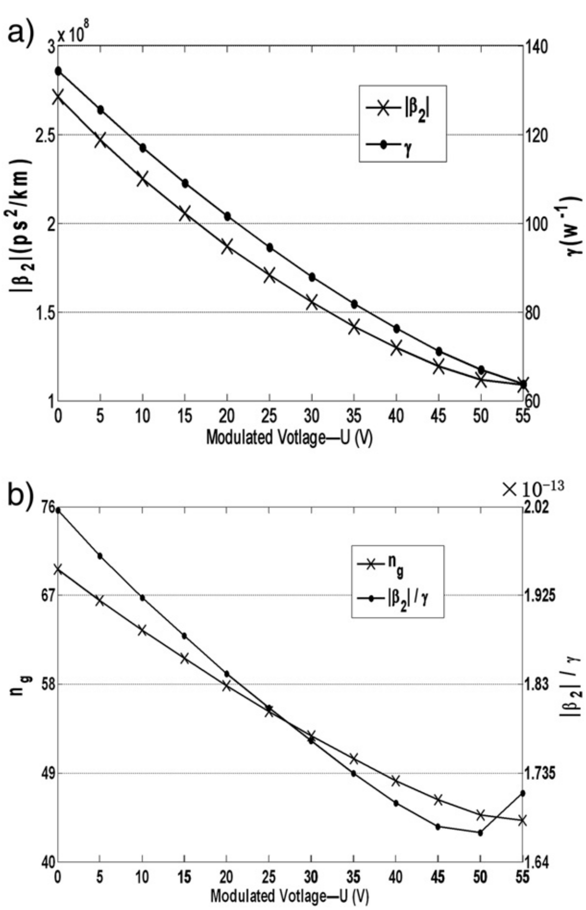

Fig. 11. (a) GVD β_2 and SPM coefficient γ as a function of applied modulated voltage; (b) n_g and $|\beta_2|/\gamma$ as a function of applied modulated voltage.

Acknowledgements

This research was supported in part by National 973 Program (No. 2012CB315705), National 863 Program (No. 2011AA010306), and NSFC (No. 60932004), PR China.

References

[1] T.F. Krauss, Journal of Physics D: Applied Physics 40 (2007) 2666.
[2] T. Baba, Nature Photonics 2 (2008) 465.
[3] F. Long, H.P. Tian, Y.F. Ji, Journal of Lightwave Technology 28 (2010) 1139.
[4] D.J. Gauthier, A.L. Gaeta, R.W. Boyd, Photonics Spectra 3 (2006) 44.
[5] T. Baba, D. Mori, Proceedings of SPIE 6351 (2006) 63511Z.
[6] J. Li, T.P. White, L. O'Faolain, A. Gomez-Iglesias, T.F. Krauss, Optics Express 16 (2008) 6227.
[7] F. Leng, W. Liang, B. Liu, T. Wang, H. Wang, Optics Express 18 (2010) 5707.
[8] R. Hao, E. Cassan, X. Le Roux, D. Gao, V. Do Khanh, L. Vivien, D. Marris-Morini, X. Zhang, Optics Express 18 (2010) 16309.
[9] M. Notomi, K. Yamada, A. Shinya, J. Takahaashi, C. Takahashi, I. Yokohama, Physical Review Letters 87 (2001) 253902.
[10] X. Zhang, H.P. Tian, Y.F. Ji, Optics Communication 283 (2010) 1768.
[11] Y. Hamachi, K. Shousaku, B. Toshihiko, Optics Letters 34 (2009) 1072.
[12] B.J. Eggleton, R.E. Slusher, C. Martijn de Sterke, P.A. Krug, J.E. Sipe, Physical Review Letters 76 (1996) 1627.
[13] B.J. Eggleton, C.M. deSterke, R.E. Slusher, Journal of the Optical Society of America B 14 (1997) 2980.
[14] B.J. Eggleton, C.M. de Sterke, R.E. Slusher, Journal of the Optical Society of America B 16 (1999) 587.
[15] C.M. de Sterke, B.J. Eggleton, Physical Review A 59 (1999) 1267.
[16] T. Kamalakis, T. Sphicopoulos, IEEE Journal of Quantum Electronics 43 (2007) 923.
[17] I. Neokosmidis, T. Kamalakis, T. Sphicopoulos, IEEE Journal of Quantum Electronics 43 (2007) 560.
[18] A. Theocharidis, T. Kamalakis, A. Chipouras, T. Sphicopoulos, IEEE Journal of Quantum Electronics 44 (2008) 1020.
[19] P. Colman, C. Husko, S. Combrie, I. Sagnes, C.W. Wong, A. De Rossi, Nature Photonics 4 (2010) 862.

[20] P. Colman, C. Husko, S. Combrié, I. Sagnes, C.W. Wong, A. De Rossi, ECOC, September 19–23 2010 Torino Italy.
[21] C. Monat, B. Corcoran, D. Pudo, M. Ebnali-Heidari, C. Grillet, M.D. Pelusi, D.J. Moss, B.J. Eggleton, et al., Journal of Selected Topics in Quantum Electronics 16 (2010) 344.
[22] Y.A. Vlasov, M. O'Boyle, H.F. Hamann, S.J. McNab, Nature 438 (2005) 65.
[23] G.P. Agrawal, Non-Linear Fiber Optics, Academic, New York, 2001.
[24] C.R. MendonCa, M.M. Costa, J.A. Giacometti, F.D. Nunes, S.C. Zilio, Electronics Letters 34 (1998) 116.
[25] A. Baron, A. Ryasnyanskiy, N. Dubreuil, P. Delaye, Q.V. Tran, G. Roosen, et al., Optics Express 17 (2009) 552.
[26] C. Husko, S. Combrié, Q.V. Tran, F. Raineri, C.W. Wong, A. De Rossi, Optics Express 17 (2009) 22442.
[27] M. Roussey, F.I. Baida, M.P. Bernal, Journal of the Optical Society of America B 24 (2007) 1416.
[28] L. Y. Liu, H. P. Tian, Y. F. Ji Acta Phys. Sin. 60 (in press).
[29] H. Rigneault, J.M. Lourtioz, C. Delalande, A. Levenson, La nanophotonique, Lavoisier, Paris, 2005.
[30] J.M. Brosi, C. Koos, L.C. Andreani, M. Waldow, J. Leuthold, W. Freude, Optics Express 16 (2008) 4177.